J|A|C|S
ARTICLES
Published on Web 07/12/2007

Separating Degenerate ^{1}H Transitions in Methyl Group Probes for Single-Quantum ^{1}H-CPMG Relaxation Dispersion NMR Spectroscopy

Vitali Tugarinov* and Lewis E. Kay*

Contribution from the Departments of Medical Genetics, Biochemistry, and Chemistry, The University of Toronto, Toronto, Ontario, Canada M5S 1A8

Received April 16, 2007; E-mail: vitali@pound.med.utoronto.ca; kay@pound.med.utoronto.ca

Abstract: A relaxation dispersion pulse scheme is presented for quantifying chemical exchange processes in proteins that exploits ^{1}H chemical shifts as probes of changes in conformation. The experiment selects ^{1}H single-quantum magnetization from the $I = {}^1/_2$ manifolds of the methyl group, which behave like AX spin systems, while suppressing coherences that derive from the ${}^3/_2$ manifold that are extremely sensitive to pulse imperfections and that would otherwise severely compromise the accuracy of the experiment. The utility of the sequence is first demonstrated with an application to a protein system that is known not to undergo chemical exchange and flat dispersion profiles are obtained. Subsequently, the methodology is applied to study the folding of a G48M mutant of the Fyn SH3 domain that has been shown previously to undergo exchange between folded and unfolded states on the millisecond time scale.

Introduction

Central to the development of NMR spectroscopy as a powerful tool for the study of molecular structure and dynamics has been the design of multipulse, multinuclear experiments that "dissect" the chemical information that is of interest from a complex network of coupled spins.[1−3] In many cases the complexities can be advantageous so long as they can be understood in detail and manipulated appropriately. One example of where this is clearly the case concerns ^{1}H−^{15}N TROSY, where interference between different relaxation mechanisms can be exploited by pulse schemes that select the most slowly relaxing multiplet component,[4] leading to improvements in spectral quality in applications involving high molecular weight proteins.[5] Our research efforts in studies of high molecular weight complexes have focused on the use of the methyl group as a probe of structure and dynamics.[6−8] Here too there is considerable complexity. In the case of a $^{13}CH_3$ moiety the energy level diagram can be written in terms of an $I = {}^3/_2$ manifold along with a pair of $I = {}^1/_2$ manifolds that include 8 ^{13}C and 10 ^{1}H single-quantum transitions that in principle can be coupled through relaxation.[9−12] The methyl group, in turn, is coupled to a network of proximal spins that can significantly alter the relaxation properties of its protons. Nevertheless, it is possible to exploit the complexity that arises from the different relaxation properties of individual methyl transitions in experiments that select specifically for slowly relaxing coherences,[13] significantly extending the range of proteins that can be studied by the NMR technique.

In what follows we provide a further example of how the complexity of a spin system can be manipulated to advantage. Here we present an experiment for the measurement of Carr−Purcell−Meiboom−Gill (CPMG[14,15]) ^{1}H relaxation dispersion profiles using $^{13}CH_3$ methyl groups that has not been possible previously.[16] Over the past several years, dating from a seminal paper by Loria and co-workers that describes how accurate X-spin CPMG relaxation dispersion profiles can be obtained for ^{1}H−X spin systems in proteins,[17] a large number of dispersion methods have been developed and applied to the study of protein folding,[18−23] enzyme function,[24−27] and bind-

(1) Wüthrich, K. *NMR of Proteins and Nucleic Acids*; John Wiley and Sons: New York, 1986.
(2) Ernst, R. R.; Bodenhausen, G.; Wokaun, A. *Principles of Nuclear Magnetic Resonance in One and Two Dimensions*; Oxford University Press: Oxford, 1987.
(3) Bax, A.; Lerner, A. *Science* **1986**, *232*, 960−967.
(4) Pervushin, K.; Riek, R.; Wider, G.; Wüthrich, K. *Proc. Natl. Acad. Sci. U.S.A.* **1997**, *94*, 12366−12371.
(5) Fiaux, J.; Bertelsen, E. B.; Horwich, A. L.; Wüthrich, K. *Nature* **2002**, *418*, 207−221.
(6) Tugarinov, V.; Hwang, P. M.; Kay, L. E. *Annu. Rev. Biochem.* **2004**, *73*, 107−146.
(7) Sprangers, R.; Kay, L. E. *Nature* **2007**, *445*, 618−622.
(8) Sprangers, R.; Gribun, A.; Hwang, P. M.; Houry, W. A.; Kay, L. E. *Proc. Natl. Acad. Sci. U.S.A.* **2005**, *102*, 16678−16683.
(9) Werbelow, L. G.; Grant, D. M. *Adv. Magn. Reson.* **1977**, *9*, 189−299.
(10) Müller, N.; Bodenhausen, G.; Ernst, R. R. *J. Magn. Reson.* **1987**, *75*, 297−334.
(11) Kay, L. E.; Prestegard, J. H. *J. Am. Chem. Soc.* **1987**, *109*, 3829−3835.
(12) Kay, L. E.; Torchia, D. A. *J. Magn. Reson.* **1991**, *95*, 536−547.
(13) Tugarinov, V.; Hwang, P. M.; Ollerenshaw, J. E.; Kay, L. E. *J. Am. Chem. Soc.* **2003**, *125*, 10420−10428.
(14) Carr, H. Y.; Purcell, E. M. *Phys. Rev.* **1954**, *4*, 630−638.
(15) Meiboom, S.; Gill, D. *Rev. Sci. Instrum.* **1958**, *29*, 688−697.
(16) Korzhnev, D. M.; Mittermaier, A.; Kay, L. E. *J. Biomol. NMR* **2005**, *31*, 337−342.
(17) Loria, J. P.; Rance, M.; Palmer, A. G. *J. Am. Chem. Soc.* **1999**, *121*, 2331−2332.
(18) Grey, M. J.; Wang, C.; Palmer, A. G. *J. Am. Chem. Soc.* **2003**, *125*, 14324−14335.
(19) Korzhnev, D. M.; Salvatella, X.; Vendruscolo, M.; DiNardo, A. A.; Davidson, A. R.; Dobson, C. M.; Kay, L. E. *Nature* **2004**, *430*, 586−590.
(20) Korzhnev, D. M.; Orekhov, V. Y.; Kay, L. E. *J. Am. Chem. Soc.* **2005**, *127*, 713−721.
(21) Korzhnev, D. M.; Neudecker, P.; Mittermaier, A.; Orekhov, V. Y.; Kay, L. E. *J. Am. Chem. Soc.* **2005**, *127*, 15602−15611.

10.1021/ja0726456 CCC: $37.00

ing.[28,29] The majority of applications have focused on studies involving X = ^{15}N or ^{13}C spin probes of dynamics. However, the use of protons can be attractive for the quantification of exchange processes in proteins because their chemical shifts can be sensitive to environment, especially when they are proximal to aromatic moieties. In this regard ^1H-methyl dispersion experiments would serve as a nice complement to existing ^{13}C-based methyl experiments,[30] so long as robust measures of exchange could be obtained. With this in mind we have designed an experiment in which magnetization derived from the $I = {}^1/_2$ methyl manifolds is targeted since it behaves in a manner analogous to magnetization originating from a simple AX spin system, for which a large number of robust CPMG dispersion experiments have been derived in the past.[21,31,32] A CPMG ^1H single-quantum (SQ) dispersion pulse scheme is presented which separates coherences from $I = {}^3/_2$ and $I = {}^1/_2$ manifolds and eliminates the former through phase cycling. Applications to a number of protein systems, including a G48M mutant of the Fyn SH3 domain that is known to exchange between folded and unfolded states on a millisecond time scale,[19] are presented, illustrating the robustness and utility of the method. We show that in certain cases more accurate ^1H chemical shift differences between exchanging states can be obtained using the methodology presented here than from an indirect method based on a simultaneous fit of methyl−^{13}C SQ and $^1H-^{13}C$ multiple-quantum (MQ) dispersion profiles that has been described previously.[16]

Materials and Methods

NMR Sample Preparation. A sample of {U-[^{15}N,^2H]; Ileδ1-[$^{13}CH_3$]; Leu, Val-[$^{13}CH_3$,$^{12}CD_3$]}-labeled B1 immunoglobulin binding domain of peptostreptoccocal protein L[33] (7.5 kDa; referred to in what follows as protein L) was prepared as described in detail previously[34,35] using U-[^2H]-D-glucose as the main carbon source and the appropriate α-keto-acid precursors for selective methyl labeling.[36] Sample conditions were as follows: 1.4 mM protein, 99.9% D_2O, 50 mM sodium phosphate, pH 6.0 (uncorrected). A sample of {U-[^{15}N,^2H]; Ileδ1-[$^{13}CH_3$]; Leu, Val-[$^{13}CH_3$,$^{13}CH_3$];^1H-Phe,Trp]}-labeled G48M Fyn SH3 was prepared as described previously.[37] Here the side chains of Phe and Trp were fully protonated (designed for a different application[37]), with all other positions in these two aromatic residues containing ^2H and ^{12}C. The protein was 1 mM in concentration, dissolved in buffer containing 90% H_2O, 10% D_2O, 50 mM sodium phosphate (pH 7.0), 0.2 mM EDTA, and 0.05% NaN_3. It is worth emphasizing the importance of highly deuterated proteins to the methodology presented below (in general we favor the labeling scheme used for protein L, described above). The use of such samples eliminates $^1H-^1H$ scalar couplings that otherwise would significantly affect the accuracy of the measurements. In addition, deuteration decreases the intrinsic transverse relaxation rates of the remaining methyl protons so that smaller dispersions can be quantified and reduces cross-relaxation pathways that can also affect the robustness of the extracted parameters.[38]

NMR Spectroscopy and Data Analysis. Studies of protein L at temperatures of 5 and 25 °C were performed at 500 MHz (^1H frequency) on a spectrometer equipped with a room-temperature probe head, while experiments on G48M Fyn SH3 were carried out at 600 MHz, 25 °C, using a spectrometer with a cryogenically cooled probe head. Spectra using the pulse scheme of Figure 2 have been obtained with 10 scans/FID, a relaxation delay of 1s and (512; 80) complex points in (t_2; t_1) giving net acquisition times of ∼30 min for each 2D data set. The SQ ^1H relaxation dispersion experiments (pulse scheme of Figure 3) have been recorded on both protein L and Fyn SH3 samples (25 °C) using a constant-time CPMG relaxation period[22] of $T = 80$ ms. Each 2D data set was recorded with 18 scans/FID, a relaxation delay of 2.0 s and (512; 80) complex points in (t_2; t_1) to give a net acquisition time of 105 min/data set. A series of 2D maps were obtained with ν_{CPMG} values varying between 50 and 1000 Hz (16 ν_{CPMG} values); two duplicate data sets were acquired for error analysis, as described previously.[19]

All NMR spectra were processed and analyzed using the NMRPipe/NMRDraw suite of programs[39] and associated software. Values of $R_{2,eff}$ have been calculated for each CPMG frequency using the relation $R_{2,eff} = -1/T \ln\{I(\nu_{CPMG})/I(0)\}$ where $I(\nu_{CPMG})$ and $I(0)$ are the intensities of cross-peaks recorded with and without the interval T, respectively.[40] Exchange parameters were extracted from fits of dispersion data to a two-site exchange model using equations that have been derived previously.[41,42] Errors in exchange parameters have been estimated from fits of two separately recorded relaxation dispersion data sets, while the errors in residue-specific parameters (such as chemical shift differences between states and intrinsic relaxation rates) have been estimated from 200 Monte Carlo simulations.[43]

Results and Discussion

Basic Problem with ^1H SQ CPMG of $^{13}CH_3$ Methyl Groups. Figure 1 shows an energy level diagram and the corresponding ^1H transitions of interest for an isolated methyl group. For simplicity, although a $^{13}CH_3$ methyl group is considered experimentally, the "^{13}C contributions" to the energy level diagram have been omitted from the figure. The spin system is most conveniently represented in terms of $I = {}^3/_2$ and a pair of $I = {}^1/_2$ manifolds;[44,45] pulses do not interconvert coherences belonging to separate manifolds, but such coherences can be coupled due to spin relaxation.[11] In the macromolecular limit and under the assumption of very rapid rotation about the methyl threefold axis the relaxation of each of the single quantum ^1H coherences, denoted by the vertical lines in Figure 1, occurs in a single-exponential manner with fast ($R^F_{2,H}$; blue

(22) Tollinger, M.; Skrynnikov, N. R.; Mulder, F. A. A.; Forman-Kay, J. D.; Kay, L. E. *J. Am. Chem. Soc.* **2001**, *123*, 11341−11352.
(23) Zeeb, M.; Balbach, J. *J. Am. Chem. Soc.* **2005**, *127*, 13207−13212.
(24) Eisenmesser, E. Z.; Millet, O.; Labeikovsky, W.; Korzhnev, D. M.; Wolf-Watz, M.; Bosco, D. A.; Skalicky, J. J.; Kay, L. E.; Kern, D. *Nature* **2005**, *3*, 117−121.
(25) Ishima, R.; Louis, J. M.; Torchia, D. A. *J. Mol. Biol.* **2001**, *305*, 515−21.
(26) Butterwick, J. A.; Loria, P. J.; Astrof, N. S.; Kroenke, C. D.; Cole, R.; Rance, M.; Palmer, A. G. *J. Mol. Biol.* **2004**, *339*, 855−871.
(27) Wang, C.; Karpowich, N.; Hunt, J. F.; Rance, M.; Palmer, A. G. *J. Mol. Biol.* **2004**, *342*, 525−537.
(28) Mulder, F. A. A.; Mittermaier, A.; Hon, B.; Dahlquist, F. W.; Kay, L. E. *Nat. Struct. Biol.* **2001**, *8*, 932−935.
(29) Tolkatchev, D.; Xu, P.; Ni, F. *J. Am. Chem. Soc.* **2003**, *125*, 12432−12442.
(30) Skrynnikov, N. R.; Mulder, F. A. A.; Hon, B.; Dahlquist, F. W.; Kay, L. E. *J. Am. Chem. Soc.* **2001**, *123*, 4556−4566.
(31) Palmer, A. G.; Kroenke, C. D.; Loria, J. P. *Methods Enzymol.* **2001**, *339*, 204−238.
(32) Palmer, A. G.; Grey, M. J.; Wang, C. *Methods Enzymol.* **2005**, *394*, 430−465.
(33) Scalley, M. L.; Yi, Q.; Gu, H.; McCormack, A.; Yates, J. R.; Baker, D. *Biochemistry* **1997**, *36*, 3373−33782.
(34) Korzhnev, D. M.; Kloiber, K.; Kanelis, V.; Tugarinov, V.; Kay, L. E. *J. Am. Chem. Soc.* **2004**, *126*, 3964−3973.
(35) Tugarinov, V.; Kay, L. E. *J. Biomol. NMR* **2004**, *29*, 369−376.
(36) Tugarinov, V.; Kanelis, V.; Kay, L. E. *Nat. Protoc.* **2006**, *1*, 749−754.
(37) Mittermaier, A.; Korzhnev, D. M.; Kay, L. E. *Biochemistry* **2005**, *44*, 15430−15436.
(38) Ishima, R.; Torchia, D. A. *J. Biomol. NMR* **2003**, *25*, 243−248.
(39) Delaglio, F.; Grzesiek, S.; Vuister, G. W.; Zhu, G.; Pfeifer, J.; Bax, A. *J. Biomol. NMR* **1995**, *6*, 277−293.
(40) Mulder, F. A. A.; Hon, B.; Muhandiram, D. R.; Dahlquist, F. W.; Kay, L. E. *Biochemistry* **2000**, *39*, 12614−12622.
(41) Carver, J. P.; Richards, R. E. *J. Magn. Reson.* **1972**, *6*, 89−105.
(42) Jen, J. *J. Magn. Reson.* **1978**, *30*, 111−128.
(43) Kamith, U.; Shriver, J. W. *J. Biol. Chem.* **1989**, *264*, 5586−5592.
(44) Corio, P. L. *Structure of High-Resolution NMR Spectra*; Academic Press: New York, 1966.
(45) Werbelow, L. G.; Marshall, A. G. *J. Magn. Reson.* **1973**, *11*, 299−313.

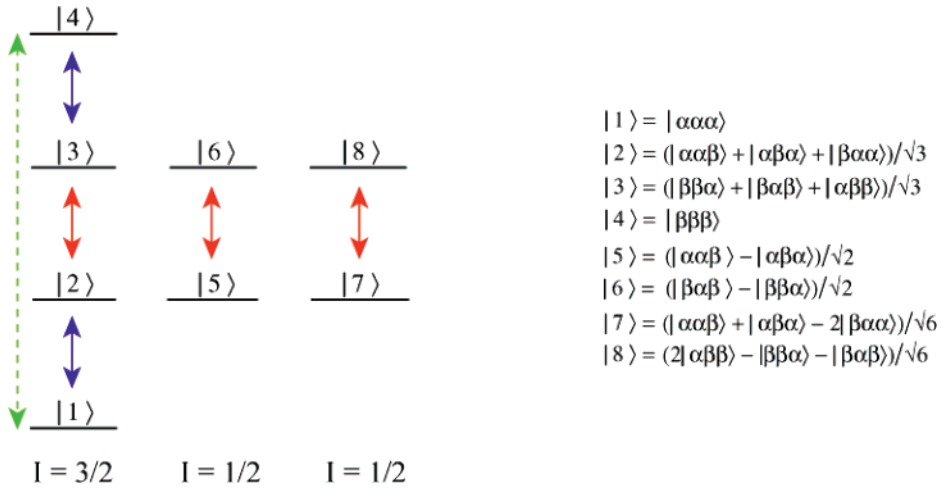

Figure 1. Energy level diagram for the X_3 spin system of a methyl group. Slow (fast) relaxing single-quantum ^{1}H transitions are shown with red (blue) arrows. The eight ^{1}H eigenstates are depicted by $|i,j,k\rangle$ ($i,j,k \in \{\alpha,\beta\}$). The spin quantum numbers, I, of the three manifolds are labeled in the diagram. Triple-quantum ^{1}H transitions are indicated by the dashed green arrow.

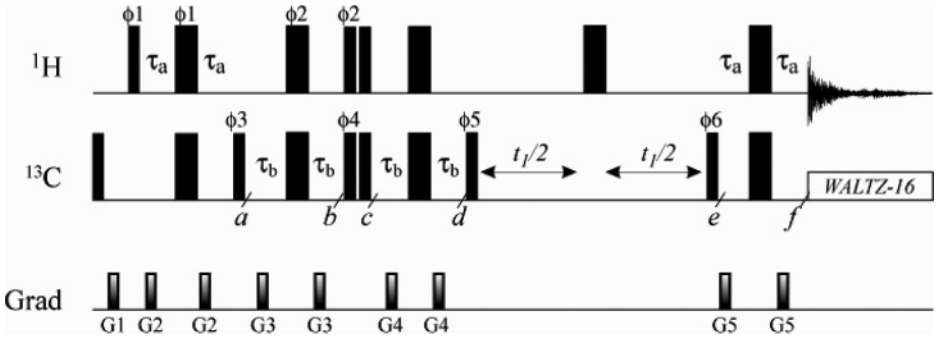

Figure 2. Pulse sequence for separation of $I = {}^1/_2$, $I = {}^3/_2$ slowly relaxing ^{1}H single-quantum transitions in $^{13}CH_3$ methyl groups. All narrow (wide) rectangular pulses are applied with flip angles of 90 (180)° along the x-axis unless indicated otherwise. The ^{1}H and ^{13}C carrier frequencies are positioned in the center of the Ileδ1-Leu-Val methyl region at 0.7 and 20 ppm, respectively. All ^{1}H and ^{13}C pulses are applied with the highest possible power, while ^{13}C WALTZ-16 decoupling[48] is achieved using a 2-kHz field. Delays are $\tau_a = 1.8$ ms; $\tau_b = 1/(8J_{HC}) = 1$ ms. The durations and strengths of pulsed-field gradients in units of (ms; G/cm) are as follows: G1 = (1; 15), G2 = (0.5; 10), G3 = (0.5; 10), G4 = (0.2; 5), G5 = (0.15; 12). The phase cycle is as follows: $\phi1 = 4(x), y$; $\phi2 = 4(y), x$; $\phi3 = 2(x,-x), x$; $\phi4 = 5(x), 5(-x)$; $\phi5 = 5(y), 5(-y)$; $\phi6 = x$; rec. $= 2(x,-x), x, 2(-x,x), -x$ (for selection of ^{1}H transitions from $I = {}^1/_2$ manifold), and $\phi1 = x, y$; $\phi2 = y, x$; $\phi3 = x, -x$; $\phi4 = 2(x), 2(-x)$; $\phi5 = 4(y), 4(-y)$; $\phi6 = x$; rec. $= x, -x, -x, x$ (for the selection of slowly relaxing ^{1}H transitions from the $I = {}^3/_2$ manifold). Quadrature detection in t_1 is achieved via STATES incrementation[49] of $\phi6$.

arrows) or slow ($R^S_{2,H}$; red arrows) rates.[10,11,13] It can be shown further (see below) that in the presence of external protons the degeneracy in the relaxation rates of the slowly relaxing ^{1}H SQ transitions (red) is lifted, with external spin contributions to the central ^{1}H transition of the $I = {}^3/_2$ manifold exceeding those to either of the two $I = {}^1/_2$ manifold ^{1}H transitions that continue to relax in an equivalent manner (see below). Differential relaxation of ^{1}H transitions, even in the absence of contributions from external spins, is the source of the problems that have plagued previous attempts to develop a ^{1}H SQ CPMG relaxation dispersion experiment for studies of methyl dynamics.[16] Any imperfections in ^{1}H 180° refocusing pulses that are applied during the CPMG pulse train leads to interchange of coherences within the $I = {}^3/_2$ manifold; because magnetization derived from the slowly relaxing transition connecting spin states |2> and |3> rapidly exceeds that from the fast decaying coherences (|3><4| and |1><2|), pulse imperfections tend to transfer magnetization from the slow to the fast relaxing coherences. Thus the effective decay rate increases with increasing numbers of refocusing pulses, even in the absence of chemical exchange, giving rise to "upward going" relaxation dispersion profiles[16] (see below). Of course, in the absence of chemical exchange flat profiles are expected.

Clearly, one solution to the problem would be to develop an experiment in which the signal from only the $I = {}^1/_2$ manifolds is detected. In this case the magnetization of interest effectively derives from AX-like spin systems, from which robust measures of dispersion can be obtained (see below). In what follows a pulse scheme for separation of signal from the $I = {}^3/_2$ and $I = {}^1/_2$ manifolds is presented, along with a description of how this is accomplished.

Pulse Scheme for Selection of ^{1}H Transitions Belonging to the $I = {}^1/_2$ Manifold. Figure 2 shows the experiment that has been developed to separate coherences from the $I = {}^3/_2$ and $I = {}^1/_2$ manifolds and to select either one or the other. At the core of the pulse sequence is the basic HMQC scheme[13,46,47] with elements that select for the slowly relaxing ^{1}H−^{13}C MQ coherences, described in detail previously.[34] In what follows, a description of the sequence is presented making use of single transition operators that provide a "feel" for how each of the transitions illustrated in Figure 1 evolves during the course of

(46) Mueller, L. *J. Am. Chem. Soc.* **1979**, *101*, 4481−4484.
(47) Bax, A.; Griffey, R. H.; Hawkings, B. L. *J. Magn. Reson.* **1983**, *55*, 301−315.
(48) Shaka, A. J.; Keeler, T.; Fenkiel, T.; Freeman, R. *J. Magn. Reson.* **1983**, *52*, 335−338.
(49) States, D. J.; Haberkorn, R.; Ruben, D. J. *J. Magn. Reson.* **1982**, *48*, 286.

the experiment. Relaxation and pulse imperfections are not included. Initially we consider the first line of the phase cycle, listed in the legend to the figure. At point *a* in the pulse scheme the coherence of interest is $\rho_a = 2I_XC_Y$, where A_Q is the $Q \in \{X,Y,Z\}$ component of A spin-angular momentum. We express $2I_XC_Y$ as

$$2I_XC_Y = 2I_X^{3/2,F}C_Y + 2I_X^{3/2,S}C_Y + 2I_X^{1/2,A}C_Y + 2I_X^{1/2,B}C_Y \quad (1)$$

where the superscript $^3/_2$ or $^1/_2$ indicates that the coherence derives from the $I = {}^3/_2$ or $I = {}^1/_2$ manifold, F or S indicates the fast or slowly relaxing coherences from the $^3/_2$ manifold (the coherences from the $^1/_2$ manifolds are slowly relaxing), and A or B distinguishes the two $I = {}^1/_2$ manifolds. Note that

$$\begin{aligned} I_X^{3/2,F} &= \sqrt{3}/2(|1><2| + |2><1| + |3><4| + |4><3|) \\ I_X^{3/2,S} &= 1(|2><3| + |3><2|) \\ I_X^{1/2,A} &= {}^1/_2(|5><6| + |6><5|) \\ I_X^{1/2,B} &= {}^1/_2(|7><8| + |8><7|) \end{aligned} \quad (2)$$

where the operators, I_Q^A, are written in terms of individual transitions, with the eigenfunctions $|j>$ defined as in Figure 1. Immediately after the $2\tau_b$ period at point *b*

$$\rho_b = -2I_{X,A}^{3/2,F}C_X + 2I_X^{3/2,S}C_Y + 2I_X^{1/2,A}C_Y + 2I_X^{1/2,B}C_Y \quad (3)$$

where

$$I_{X,A}^{3/2,F} = \sqrt{3}/2(|1><2| + |2><1| - |3><4| - |4><3|) \quad (4)$$

The phase of the subsequent ^{13}C 90° pulse is cycled $\pm x$, with concomitant inversion of the receiver phase, so that $-2I_{X,A}^{3/2,F}C_X$ is eliminated. At point *c* the density matrix of interest, ρ_c, is given by

$$\begin{aligned} \rho_c = &-1/2\ 2I_Y^{3/2,F}C_Y - 1/4\ 2I_Y^{3/2,S}C_Y - 2I_Y^{1/2,A}C_Y - 2I_Y^{1/2,B}C_Y \\ &-3i/2\ |1><4|C_Y + 3i/2|4><1|C_Y \end{aligned} \quad (5)$$

where

$$\begin{aligned} I_Y^{3/2,F} &= -\sqrt{3}\ i/2(|1><2| - |2><1| + |3><4| - |4><3|) \\ I_Y^{3/2,S} &= -i(|2><3| - |3><2|) \\ I_Y^{1/2,A} &= -i/2(|5><6| - |6><5|) \\ I_Y^{1/2,B} &= -i/2(|7><8| - |8><7|) \end{aligned} \quad (6)$$

The $|1><4|$ and $|4><1|$ elements in eq 5 are ^1H triple-quantum coherences that persist through the remainder of the pulse scheme and cannot be detected; in what follows we neglect them. The subsequent $2\tau_b$ period produces

$$\rho_d = -{}^1/_2\ 2I_{Y,A}^{3/2,F}C_X - {}^1/_4\ 2I_Y^{3/2,S}C_Y - 2I_Y^{1/2,A}C_Y - 2I_Y^{1/2,B}C_Y \quad (7)$$

where

$$I_{Y,A}^{3/2,F} = \sqrt{3}\ i/2(|1><2| - |2><1| - |3><4| + |4><3|) \quad (8)$$

and as before $2I_{Y,A}^{3/2,F}C_X$ is eliminated by the application of the ^{13}C $90_{\phi 5}$ pulse and the associated phase cycling. Subsequently, magnetization evolves for t_1, during which time ^{13}C chemical shift is recorded. Antiphase ^1H magnetization is refocused during the $2\tau_a$ period between *e* and *f*, and at the start of acquisition the signal of interest is proportional to

$$\rho_{f,1-4} = {}^1/_4\ I_X^{3/2,S} + I_X^{1/2,A} + I_X^{1/2,B} \quad (9)$$

where the subscript $1-4$ denotes the fact that the acquired signal is the same for each of the phase cycle steps $1-4$ (see legend to Figure 2). By contrast, for scan 5

$$\rho_{f,5} = -I_X^{3/2,S} - I_X^{1/2,A} - I_X^{1/2,B} \quad (10)$$

Thus, magnetization derived from the $I = {}^1/_2$ manifold can be isolated by the linear combination $4\rho_{f,1-4} + \rho_{f,5}$, while slowly relaxing magnetization exclusively from the $I = {}^3/_2$ manifold is obtained by considering the following combination, $\rho_{f,1} + \rho_{f,5}$.

It is of interest to calculate the intensities of correlations in experiments that select for slowly relaxing single-quantum ^1H coherences from either $I = {}^1/_2$ or $I = {}^3/_2$ manifolds ($S^{1/2}$or $S^{3/2}$) relative to intensities of cross-peaks in $^1H-^{13}C$ HMQC correlation maps where only the slowly decaying components of magnetization are chosen, $S^{HMQC,S}$. The ratio $S^{1/2}/S^{HMQC,S}$ is given by

$$\begin{aligned} Tr\{(4\rho_{f,1-4} + \rho_{f,5})(I_X^{3/2,S} + I_X^{1/2,A} + I_X^{1/2,B})\}/ \\ \{5Tr(I_X^{3/2,S} + I_X^{1/2,A} + I_X^{1/2,B})^2\} = {}^1/_5 \end{aligned} \quad (11)$$

where the factor of 5 in the denominator takes into account the 5 scans that are recorded to isolate the $^1/_2$ manifold and "Tr" refers to the trace of the matrix. It is worth noting that a sensitivity-enhanced version of the sequence of Figure 2 that selects for the $I = {}^1/_2$ manifold has been developed that improves the signal-to-noise by a factor of $\sqrt{2}$ (not shown). In a similar manner,

$$\begin{aligned} S^{3/2}/S^{HMQC,S} = Tr\{(\rho_{f,1-4} + \rho_{f,5})(I_X^{3/2,S} + I_X^{1/2,A} + I_X^{1/2,B})\}/ \\ \{2Tr(I_X^{3/2,S} + I_X^{1/2,A} + I_X^{1/2,B})^2\} = -{}^1/_4 \end{aligned} \quad (12)$$

where the factor of 2 in the denominator accounts for the fact that two scans are required to select for signal from the $^3/_2$ manifold; in this case we have not been able to design a sensitivity-enhanced version. It is clear that there is a considerable sensitivity penalty associated with manifold selection; nevertheless, as we show below, high quality spectra can be recorded in very reasonable measuring times, at least for small to medium sized proteins.

In order to verify that the pulse scheme of Figure 2 selects the proper components of magnetization we initially performed a number of qualitative "checks". First, the ratios $S^{1/2}/S^{HMQC,S}$ and $S^{3/2}/S^{HMQC,S}$ have been measured for 15 methyl peaks of {U-[^{2}H]; Ileδ1-[$^{13}CH_3$]; Leu,Val-[$^{13}CH_3$,$^{12}CD_3$]}-labeled protein L. Values of 0.21 ± 0.01 and 0.20 ± 0.01 were obtained that are in reasonable agreement with the factors of $^1/_5$ and $^1/_4$ that are predicted in the absence of relaxation and pulse imperfec-

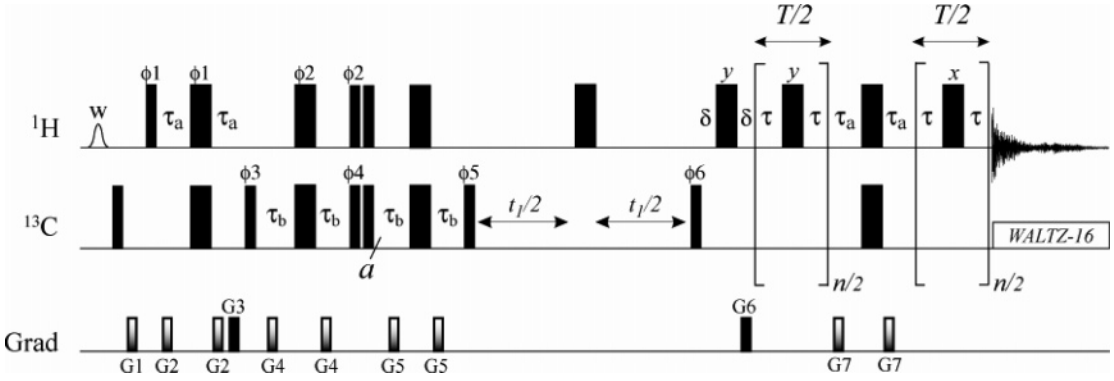

Figure 3. Pulse scheme for the measurement of ^{1}H CPMG SQ relaxation dispersion profiles of methyl groups. All parameters are as in the legend to Figure 2; $\delta = 1$ ms, $\tau_a = 1/(4J_{HC})$. The strengths and durations of pulsed-field gradients in units of (ms; G/cm) are as follows: G1 = (1; 15); G2 = (0.5; 10); G3 = (0.5; 30); G4 = (0.5; 10); G5 = (0.2; 5); G6 = (0.5; 30); G7 = (0.15; 5). The phase cycle is as follows: $\phi1 = 8(x), y$; $\phi2 = 8(y), x$; $\phi3 = 4(x,-x), x$; $\phi4 = 9(x), 9(-x)$; $\phi5 = 9(y), 9(-y)$; $\phi6 = x$; rec. $= 4(x,-x), x, 4(-x,x), -x$. The shaped pulse marked with "w" is implemented as a water-selective ~7 ms EBURP-1 pulse.[52] Quadrature detection in t_1 is achieved using STATES[49] incrementation of $\phi6$. See Materials and Methods for additional details. $n/2$ is even.

tions. Very similar ratios were also obtained in studies of the Fyn-SH3 domain, discussed below.

As a second check, the transverse relaxation rates of slowly relaxing ^{1}H magnetization derived (i) from *both* $I = {}^3/_2$ and $I = {}^1/_2$ manifolds, $R_2^S = R_2(I_X^{3/2,S} + I_X^{1/2,A} + I_X^{1/2,B})$, (ii) from the $I = {}^1/_2$ manifold, $R_2^{S,1/2} = R_2(I_X^{1/2,A} + I_X^{1/2,B})$, and (iii) from the $I = {}^3/_2$ manifold, $R_2^{S,3/2} = R_2(I_X^{3/2,S})$, have been measured by quantifying the initial decay rates of magnetization and subsequently compared. As described in some detail in previous publications,[50,51] the relaxation of ^{1}H single-quantum coherences derived from each of the transitions in Figure 1 can be modeled by

$$\frac{d\vec{v}(t)}{dt} = -(\tilde{D} + \tilde{E})\,\vec{v}(t) \qquad (13)$$

where $\tilde{D} = diag(R_{2,H}^F, R_{2,H}^S, R_{2,H}^F, R_{2,H}^S, R_{2,H}^S)$ is a diagonal matrix that accounts for relaxation contributions that arise from interactions within the methyl spin system, the matrix $\tilde{E}$ accounts for the external protons, $\vec{v}^{,T} = (|1><2|,|2><3|,|3><4|, |5><6|,|7><8|)$, and the superscript T denotes transpose. Here

$$\tilde{E} = k_{HH}\begin{bmatrix} 9 & -2\sqrt{3} & 0 & 0 & 0 \\ -2\sqrt{3} & 11 & -2\sqrt{3} & 0 & 0 \\ 0 & -2\sqrt{3} & 9 & 0 & 0 \\ 0 & 0 & 0 & 5 & 0 \\ 0 & 0 & 0 & 0 & 5 \end{bmatrix},$$

$$k_{HH} = \sum_{ext}\left(\frac{1}{20}\right)\frac{\hbar^2\gamma_H^4\tau_C}{r_{HHext}^6} \qquad (14)$$

where τ_C is the correlation time of the assumed isotropically rotating protein and r_{HHext} is the distance between a methyl proton and a proton external to the methyl group in question. The summation in eq 14 is over all external protons. In the derivation of eq 14 cross-correlation effects between different external spin interactions involving a single methyl site are not included; however, for each external proton-methyl group interaction, dipolar cross-correlations are accounted for. Focusing only on the diagonal elements of eq 14 it is clear that the effect of external protons is to increase $R_2^{S,3/2}$ relative to $R_2^{S,1/2}$ ($R_2^{S,3/2} > R_2^{S,1/2}$).

Values of $R_2^{S,1/2}$ and $R_2^{S,3/2}$ have been measured using a very slightly modified version of the sequence of Figure 2. Since the fast relaxing ^{1}H SQ coherences $|1><2|$ and $|3><4|$ are eliminated prior to the delay during which the relaxation rates are quantified, the initial decay of magnetization is single-exponential with decay constants of $R_2^{S,1/2} = R_{2,H}^S + 5k_{HH}$ and $R_2^{S,3/2} = R_{2,H}^S + 11k_{HH}$. Average free-precession relaxation rates in protein L(Fyn SH3) at 25 °C are $R_2^{S,1/2} = 4.9 \pm 1.3\ s^{-1}$ and $R_2^{S,3/2} = 6.7 \pm 1.1\ s^{-1}$ ($13.2 \pm 7.3\ s^{-1}$, $15.6 \pm 8.1\ s^{-1}$), with the higher rates for the SH3 domain reflecting to a large extent the contributions from chemical exchange that elevate the free precession relaxation rates in this sample and to a much smaller extent the higher levels of protonation (see Materials and Methods). For each Ile, Leu, and Val site in the two proteins examined, $R_2^{S,3/2} > R_2^{S,1/2}$ as expected. We have also measured R_2^S (see above) and for all Ile, Leu, and Val residues in both proteins $R_2^{S,1/2} < R_2^S < R_2^{S,3/2}$, that is in keeping with eq 14 above. Finally, statistically significant correlations are obtained between $R_2^{S,3/2} - R_2^{S,1/2}$ and $(\sum_{ext} 1/r_{HHext}^6)$ with Pearson correlation coefficients of 0.71(0.60) for 13 well-resolved methyl peaks in protein L at 5 °C (25 °C).

A ^{1}H SQ Relaxation Dispersion Experiment for Methyl Groups. As described above a number of qualitative tests have been performed to establish that separation of magnetization from $I = {}^3/_2$ and $I = {}^1/_2$ manifolds can be achieved. However, the ultimate test would be to develop a ^{1}H dispersion experiment based on the ideas presented above (Figure 2) and show that flat dispersion profiles are obtained in applications to samples that are devoid of chemical exchange. Figure 3 illustrates such an experiment. The sequence is essentially identical to that presented in Figure 2 for manifold separation with the exception that a constant-time CPMG element[22] is inserted prior to acquisition that modulates the effects of exchange for millisecond time-scale dynamic processes. In addition, a pair of gradients have been inserted, G3 and G6, that select against the ^{1}H triple-quantum coherences that are present by point *a* in the scheme. As described above, in the absence of pulse

(50) Tugarinov, V.; Kay, L. E. *J. Am. Chem. Soc.* **2006**, *128*, 7299−7308.
(51) Tugarinov, V.; Sprangers, R.; Kay, L. E. *J. Am. Chem. Soc.* **2007**, *129*, 1743−1750.
(52) Geen, H.; Freeman, R. *J. Magn. Reson.* **1991**, *93*, 93−141.

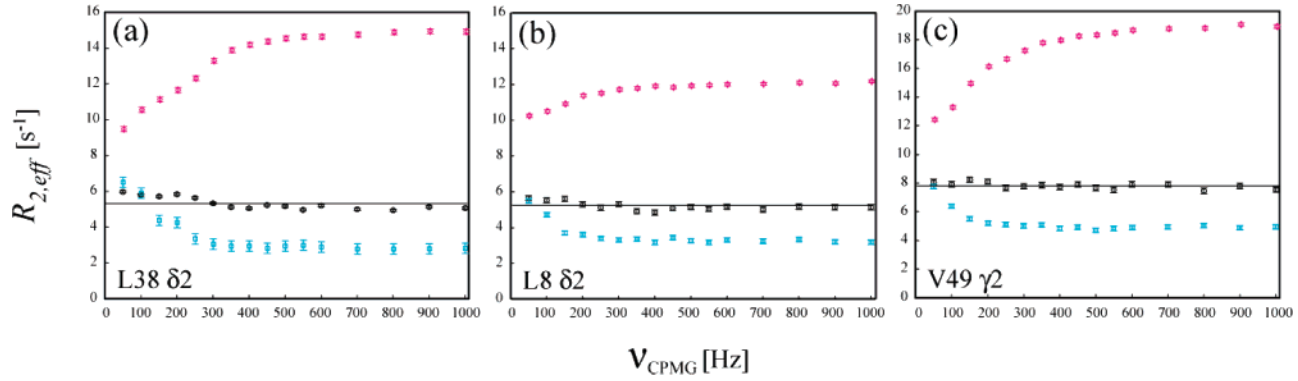

Figure 4. ^{1}H-methyl CPMG relaxation dispersion profiles for selected methyl groups of {U-[^{2}H]; Ileδ1-[$^{13}CH_3$]; Leu,Val-[$^{13}CH_3$,$^{12}CD_3$]}-labeled protein L, 5 °C, 500 MHz. Curves in red show $R_{2,eff}$ vs ν_{CPMG} for the sum of slowly relaxing ^{1}H SQ components from both $I = {}^3/_2$ and $I = {}^1/_2$ manifolds; blue curves were obtained from the scheme of Figure 3 with G3 = G6 = 0 (with appropriate adjustment of phase cycle as in Figure 2) that does not eliminate triple-quantum coherences; black curves were generated from the sequence of Figure 3 with G3 and G6 set to select SQ magnetization. The solid black lines are the best fit of the data to $R_{2,eff} = k$. Note that the red profile for the L8 δ2 site is the least "upward going" of the three; this residue is the most disordered methyl-bearing side chain in protein L with the smallest difference between $R^F_{2,H}$ and $R^S_{2,H}$.[16]

imperfections these coherences are not converted to observable magnetization. However, the refocusing pulses of the CPMG element are not perfect, and it is expected that there will be some conversion of triple- to observable single-quantum magnetization in a manner that depends on the number of refocusing pulses (see below). Note that pulse imperfections can also lead to conversion between fast and slowly relaxing coherences within the $I = {}^3/_2$ manifold but such effects are "subtracted out" by the phase cycling scheme which suppresses magnetization components that derive from this manifold. It can be shown that the application of gradients G3/G6 eliminates $^1/_2$ of the magnetization of interest in the case that phase $\phi 2 = y$ in the scheme of Figure 3; this is accounted for by adjusting the number of scans accordingly, as described in the legend to this figure. Figure 4 shows relaxation dispersion profiles measured on a sample of {Ileδ1-[$^{13}CH_3$]; Leu,Val-[$^{13}CH_3$,$^{12}CD_3$]}-labeled protein L that does not show evidence of exchange from both ^{15}N relaxation dispersion and methyl ^{13}C relaxation dispersion experiments,[34] where flat profiles are obtained. The red profiles are those obtained using a pulse scheme where no attempt is made to separate ^{1}H coherences from $I = {}^3/_2$ and $I = {}^1/_2$ manifolds, and as described briefly above and in more detail previously,[16] the interconversion between fast and slowly relaxing ^{1}H lines in the $^3/_2$ manifold resulting from pulse imperfections in the CPMG element leads to "upward going" dispersion profiles. Alternatively, if the scheme of Figure 3 is employed, but with gradients G3 and G6 removed, dispersion profiles are obtained (blue) that are easily mistaken as being derived from exchange. Dispersion profiles obtained from the experiment of Figure 3 (with gradients G3/G6 $\neq$ 0) are illustrated in black, along with best fit horizontal lines, and it is clear that much flatter "curves" are obtained in this case. The pairwise rmsd, $RMSD = \sqrt{N^{-1}\sum_i\{R^i_{2,eff}(\nu_{CPMG,i}) - k\}^2}$ where $R^i_{2,eff}$ is the effective transverse relaxation rate at CPMG frequency $\nu_{CPMG,i}$, $R_{2,eff}(\nu_{CPMG}) = k$, is the best fit horizontal line to the experimental curve, and N is the number of data points in the dispersion profile has been computed for each dispersion (generated from the sequence of Figure 3 with G3/G6 $\neq$ 0), and an average value of $RMSD = 0.30 \pm 0.05$ s^{-1} is obtained, with a maximum value of 0.49 s^{-1}. These values of *RMSD* are similar to those obtained in experiments that measure heteronuclear SQ dispersion rates on protein systems that do not show exchange. We have also quantified the difference in relaxation rates obtained for the lowest and highest ν_{CPMG} values, $R_{ex} = R_{2,eff}(50\text{ Hz}) - R_{2,eff}(1000\text{ Hz})$. For the 15 residues that were examined R_{ex} varies from 0.11 to 1.36 s^{-1}, with an average of 0.73 s^{-1} and a standard deviation of 0.36 s^{-1}; for only 2 residues was R_{ex} in excess of 1 s^{-1}. Thus, we recommend that dispersion profiles only be quantified in cases where $R_{ex} > 2-3$ s^{-1}. Indeed, in the analysis of exchange in the Fyn SH3 domain considered below, dispersion curves were only considered when $R_{ex} > 4$ s^{-1}.

Application to Folding of a G48M Mutant Fyn SH3 Domain. In a previous series of publications[19,21,37,53,54] we have shown that the SH3 domain from the Fyn tyrosine kinase folds on the millisecond time scale and that ^{15}N and ^{13}C CPMG relaxation dispersion NMR spectroscopy can provide detailed information about the kinetics and thermodynamics of the folding reaction along with structural information about the excited states that form along the folding pathway. We show here that methyl-^{1}H CPMG relaxation dispersion can also be used as a valuable probe in this system. Figure 5a shows the two-dimensional ^{1}H$-^{13}$C methyl correlation map of the {U-[^{15}N,^{2}H]; Ileδ1-[$^{13}CH_3$]; Leu,Val-[$^{13}CH_3$,$^{13}CH_3$];^{1}H-Phe,Trp]}-labeled G48M mutant Fyn SH3 domain (G48M Fyn SH3), 500 MHz, 25 °C, recorded using the pulse-scheme of Figure 3 with $T = 0$. As discussed in Materials and Methods, a highly deuterated sample has been employed in this study to eliminate ^{1}H$-^1$H scalar couplings and to minimize cross-relaxation that could otherwise affect dispersion profiles.[38] Figure 5b–f show the ^{1}H SQ relaxation dispersion profiles obtained at 600 MHz, 25 °C, for the five most upfield-shifted methyl resonances of G48M Fyn-SH3. All 12 ^{1}H SQ profiles that derive from well separated peaks, and for which $R_{ex} = R_{2,eff}(50\text{ Hz}) - R_{2,eff}(1000\text{ Hz}) > 4\text{s}^{-1}$, were fit simultaneously to a two-site model of folding, $U \underset{k_U}{\overset{k_F}{\rightleftharpoons}} F$, and values of $k_{ex} = k_F + k_U = 472 \pm 38$ s^{-1} and $p_U = 3.8 \pm 0.1\%$ (the population of the invisible unfolded state, U) were obtained. These values are in reasonable agreement with $k_{ex} = 418 \pm 6$ s^{-1} and $p_U = 4.2 \pm 0.1\%$ that were reported previously based on a simultaneous fit of ^{13}C SQ and ^{1}H$-^{13}$C

(53) Orekhov, V. Y.; Korzhnev, D. M.; Kay, L. E. *J. Am. Chem. Soc.* **2004**, *126*, 1886–1891.
(54) Korzhnev, D. M.; Neudecker, P.; Zarrine-Afsar, A.; Davidson, A. R.; Kay, L. E. *Biochemistry* **2006**, *45*, 10175–10183.

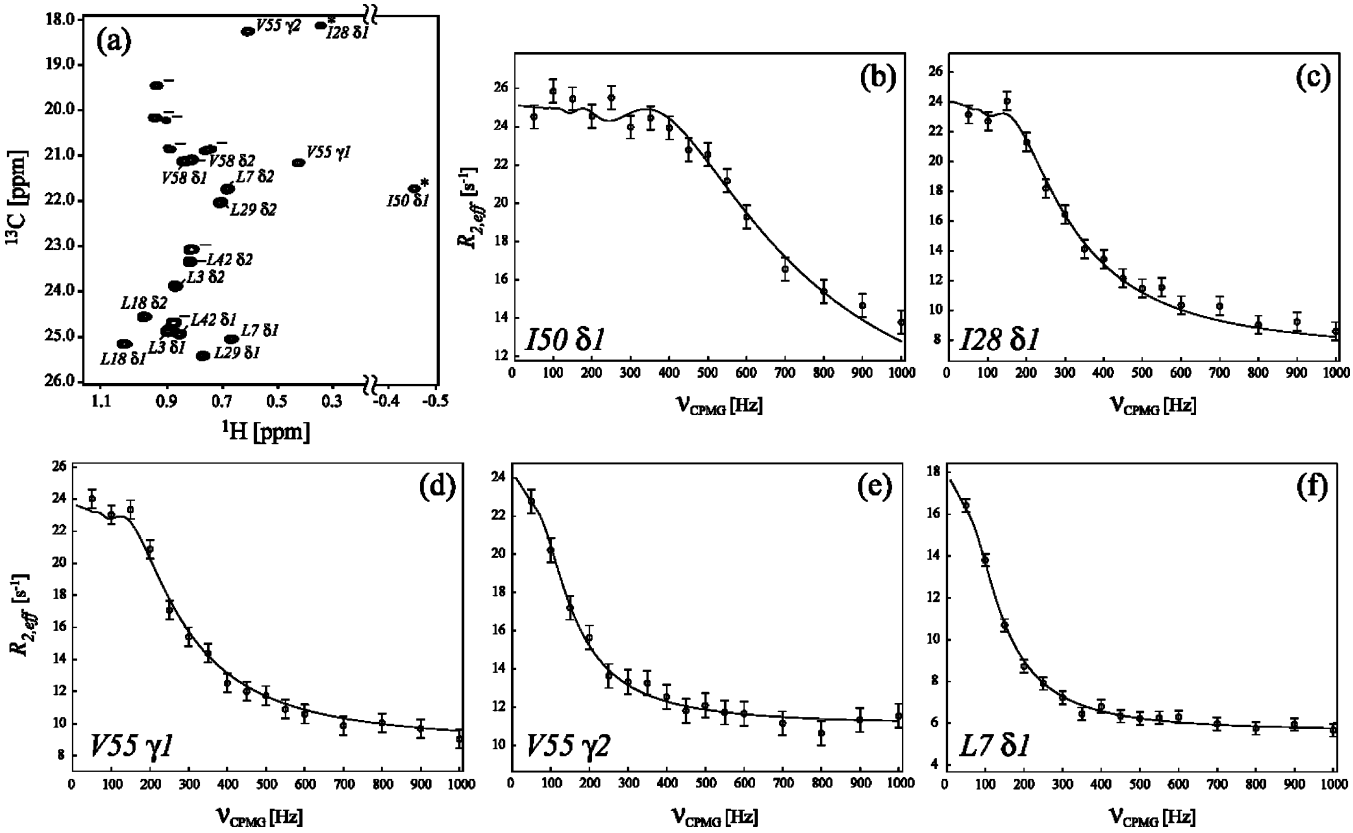

Figure 5. (a) 2D methyl $^{1}H-^{13}C$ correlation map of the {U-[^{15}N,^{2}H]; Ileδ1-[$^{13}CH_3$]; Leu,Val-[$^{13}CH_3$,$^{13}CH_3$];^{1}H-Phe,Trp]}-labeled Fyn SH3 domain obtained using the pulse scheme of Figure 3 with $T = 0$, 500 MHz, 25 °C. The peaks marked with asterisks are aliased in the ^{13}C dimension, while those denoted by "−" derive from residues that belong to tags that are beyond the structured region of the domain and were excluded from all analyses. (b−f) ^{1}H SQ relaxation dispersion profiles (600 MHz, 25 °C) obtained for the five most upfield methyl resonances in (a). The solid lines correspond to fits of the dispersion data (all dispersion curves are fit "globally") to a model of two-site chemical exchange (see text).

MQ data to the same two-site exchange model.[16] The slight difference in values may well reflect the fact that the exchange process is, in fact, three-site, with the formation of an on-pathway folding intermediate.[19] Our previous studies that made use of methyl group probes showed that the chemical shifts of the methyl carbons in the intermediate state were essentially random-coil-like and hence very similar to those of the *U* state so that a two-site exchange model could fit the data well. In contrast, ^{15}N dispersion data could only be properly fit to a more complex three-site exchange model.[19] It may be that the intermediate state ^{1}H shifts are distinct from the *U* state shifts, such as for ^{15}N, so that the ^{1}H-methyl data only approximates two-site exchange. If this is the case then some difference between exchange parameters obtained using the different probes would be expected for the simplistic two-site fit. In this regard it is of interest to note that the reduced χ^2 value obtained from fits of the ^{1}H CPMG data is 2, somewhat higher than what was obtained in the analysis of the ^{13}C SQ/$^{1}H-^{13}C$ MQ dispersion data, 0.6.[16] A deeper understanding of the ^{1}H dispersion data will require a temperature dependent study and experiments at several field strengths and is beyond the scope of the present work.

Values of $|\Delta\varpi_H|$ (in ppm) extracted from the "global" fit of the ^{1}H SQ relaxation data with $k_{ex}(p_U)$ fixed to 472 s^{-1}(3.8%) are listed in Table 1 together with the earlier reported values of $|\Delta\varpi_H|$ obtained from a combined set of ^{13}C SQ and $^{1}H-^{13}C$ MQ data.[16] In general, $|\Delta\varpi_H|$ values are in good agreement, with significant discrepancies noted only for Ile50 δ1 and Val55 γ1, both with large $|\Delta\varpi_H|$ (Pearson's $R = 0.983$ between the two sets upon exclusion of these two residues). It has been established that $^{1}H-^{13}C$ MQ dispersion profiles are significantly attenuated for large $|\Delta\varpi_H|$ and can even increase with ν_{CPMG}.[34,55]

Table 1. Comparison of ^{1}H Chemical Shift Differences between Exchanging Sites, $|\varpi_H|$, in G48M Fyn SH3 Extracted from (i) a "Global" Fit of a Combined Set of ^{13}C SQ/$^{1}H-^{13}C$ MQ Dispersion Profiles[16] and from (ii) ^{1}H SQ Methyl Dispersion Profiles[a]

residue	$\lvert\varpi_H\rvert$[b]	$\lvert\varpi_H\rvert$[c]
Leu 3 δ1	0.06 ± 0.002	0.08 ± 0.020
Leu 3 δ2	0.09 ± 0.002	0.11 ± 0.002
Leu 7 δ1	0.15 ± 0.006	0.19 ± 0.001
Leu 7 δ2	0.09 ± 0.002	0.10 ± 0.002
Leu 18 δ1	0.11 ± 0.007	0.18 ± 0.001
Leu 18 δ2	0.14 ± 0.003	0.17 ± 0.003
Ile 28 δ1	0.43 ± 0.006	0.49 ± 0.010
Leu 29 δ1	0.07 ± 0.001	0.08 ± 0.001
Leu 29 δ2	0.07 ± 0.001	0.09 ± 0.001
Leu 42 δ1	0	0.04 ± 0.030[d]
Leu 42 δ2	0	0.03 ± 0.001[d]
Ile 50 δ1	0.13 ± 0.003	1.11 ± 0.020
Val 55 γ1	0.09 ± 0.008	0.43 ± 0.020
Val 55 γ2	0.17 ± 0.005	0.23 ± 0.010
Val 58 γ1	0.06 ± 0.004	−*,[d]
Val 58 γ2	0.09 ± 0.002	0.08 ± 0.010* [d]

[a] All chemical shifts are given in ppm; the peaks of Val58 marked with asterisks overlap, and the value of $|\varpi_H|$ reported for γ2 is derived from the combined peak. [b] $|\varpi_H|$ obtained from the "global" fit of the combined set of ^{13}C SQ and $^{1}H-^{13}C$ MQ data;[16] [c] $|\varpi_H|$ obtained from the "global" fit of the ^{1}H SQ data. [d] Residues that were not included in the subset used to derive global k_{ex} and p_U parameters.

(55) Korzhnev, D. M.; Kloiber, K.; Kay, L. E. *J. Am. Chem. Soc.* **2004**, *126*, 7320−7329.

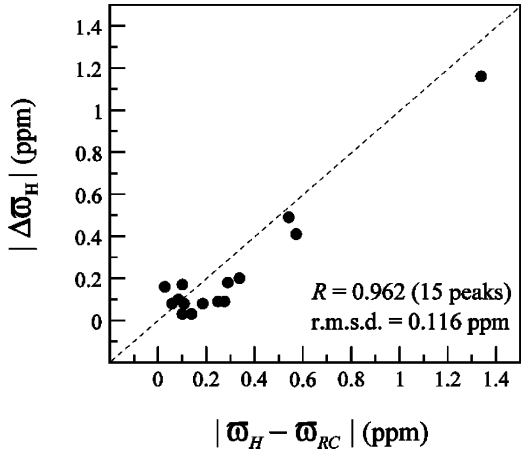

Figure 6. Linear correlation plot of $|\Delta\varpi_H|$, *y*-axis, and the calculated difference between the measured ^1H chemical shift of a given methyl in the folded state, ϖ_H, and its random-coil value,[56] ϖ_{RC}, *x*-axis. The Pearson correlation coefficient *R* and the pairwise rmsd between the two data sets are shown.

It can, therefore, be difficult to extract accurate ^1H shift differences in these cases, unless high sensitivity data are obtained. In contrast, accurate values of $|\Delta\varpi_H|$ are more readily obtained from SQ ^1H CPMG experiments that provide a direct measure of such chemical shift differences in the first place.

Figure 6 shows the correlation between values of $|\Delta\varpi_H|$, and the calculated differences $|\varpi_H - \varpi_{RC}|$, where ϖ_H is the folded state chemical shift (measured from Figure 5a) and ϖ_{RC} is the methyl-specific ^1H random-coil chemical shift[56] that to first approximation represents the chemical shift of the methyl group in the unfolded state. In contrast to the $|\Delta\varpi_H|$ values for Ile50 $\delta1$ and Val55 $\gamma1$ that have been obtained previously from the "global" fit of ^{13}C SQ and $^1H-^{13}C$ MQ dispersion profiles[16] and that do not correlate well with $|\varpi_H - \varpi_{RC}|$, the $|\Delta\varpi_H|$ values obtained directly from ^1H SQ dispersion measurements for these residues are consistent with the calculated values of $|\varpi_H - \varpi_{RC}|$ (see Table 1 and Figure 6). A more careful analysis of the ^{13}C SQ and $^1H-^{13}C$ MQ data shows that for these two residues $|\Delta\varpi_H|$ is not well determined and that $|\Delta\varpi_H|$ values obtained from the ^1H relaxation dispersion experiment presented here are equally consistent with the MQ dispersion profiles. Interestingly, methyl groups from residues Ile 28, Ile 50, and Val 55 that have the largest values of $|\Delta\varpi_H|$, Table 1, form a "cluster" with each methyl close to at least one aromatic ring (normally several).

Finally, it is worth pointing out that it is also possible to record ^1H methyl SQ CPMG relaxation dispersion profiles on highly deuterated samples where Ile($\delta1$), Leu, and Val methyl groups are labeled as $^{13}CHD_2$ using a pulse scheme that is very similar to those already proposed for recording ^{13}C or ^{15}N dispersion experiments on AX spin systems. These samples are readily produced since the precursors necessary for "$^{13}CHD_2$ enrichment" are available commercially. Previously we have shown that $^1H-^{13}C$ correlation spectra recorded on highly deuterated malate synthase G (82 kDa) samples that were labeled as $^{13}CH_3$ were a factor of 3−4 more sensitive than the corresponding spectra measured on samples that contained the $^{13}CHD_2$ isotopomer.[57] Thus, it is expected that dispersion spectra for $^{13}CHD_2$-labeled samples would be between 2- and 3-fold more sensitive than those recorded using the scheme that is presented here for the $^{13}CH_3$ methyl isotopomer, when the sensitivity losses that accompany this experiment are taken into account (see discussion above and summary below). Nevertheless, the choice of what labeling scheme to use, $^{13}CH_3$ or $^{13}CHD_2$, depends to a large extent on what other experiments might be performed with the sample; in our laboratory we make use of $^{13}CH_3$-labeling for a variety of applications,[51,58,59] so that the ^1H-dispersion scheme presented here will be of particular value.

In summary, we have presented an experiment for the measurement of ^1H methyl SQ CPMG relaxation dispersion profiles that is based on magnetization derived exclusively from the slowly relaxing $I = {}^1/_2$ manifold coherences. Correlations in the dispersion experiment (for $T = 0$, Figure 3) are on average a factor of 9 less sensitive than the corresponding cross-peaks in a methyl TROSY $^1H-^{13}C$ data set that selects for all of the slowly relaxing coherences (this includes the factor of 2 sensitivity loss due to the application of the SQ selection gradients). Nevertheless, high quality data sets can be recorded in 1−2 h for the 1 mM samples studied here, and it is likely, therefore, that the methodology will be applicable to most proteins with molecular masses up to 20 kDa. The ^1H CPMG experiment will be a useful complement to existing methyl ^{13}C SQ and $^1H-^{13}C$ MQ CPMG pulse schemes that probe slow conformational exchange in the hydrophobic cores of proteins.

Acknowledgment. The authors thank Dr. Dmitry Korzhnev (University of Toronto) for useful discussions. This work was supported by grants from the Canadian Institutes of Health Research and the Natural Sciences and Engineering Research Council of Canada. L.E.K. is the recipient of a Canada Research Chair in Biochemistry.

JA0726456

(56) Wishart, D. S.; Bigam, C. G.; Holm, A.; Hodges, R. S.; Sykes, B. D. *J. Biomol. NMR* **1995**, *5*, 67−81.
(57) Ollerenshaw, J. E.; Tugarinov, V.; Skrynnikov, N. R.; Kay, L. E. *J. Biomol. NMR* **2005**, *33*, 25−41.
(58) Tugarinov, V.; Kay, L. E. *ChemBioChem* **2005**, *6*, 1567−1577.
(59) Tugarinov, V.; Choy, W. Y.; Orekhov, V. Y.; Kay, L. E. *Proc. Natl. Acad. Sci. U.S.A.* **2005**, *102*, 622−627.